

Semiexperimental Equilibrium Structure for the C₆ Backbone of *cis*-1,3,5-Hexatriene; Structural Evidence for Greater π -Electron Delocalization with Increasing Chain Length in Polyenes

Richard D. Suenram,[†] Brooks H. Pate,[†] Alberto Lesarri,[‡] Justin L. Neill,[†] Steven Shipman,[†] Robin A. Holmes,[§] Matthew C. Leyden,[§] and Norman C. Craig^{*,§}

Department of Chemistry, University of Virginia, Charlottesville, Virginia 22904, Departamento de Química Física y Química Inorgánica, Universidad de Valladolid, Valladolid, Spain 47005, and Department of Chemistry and Biochemistry, Oberlin College, Oberlin, Ohio 44074

Received: December 4, 2008; Revised Manuscript Received: December 30, 2008

Twenty-five microwave lines were observed for *cis*-1,3,5-hexatriene (0.05 D dipole moment) and a smaller number for its three ¹³C isotopomers in natural abundance. Ground-state rotational constants were fitted for all four species to a Watson-type rotational Hamiltonian for an asymmetric top ($\kappa = -0.9768$). Vibration–rotation (alpha) constants were predicted with a B3LYP/cc-pVTZ model and used to adjust the ground-state rotational constants to equilibrium rotational constants. The small inertial defect for *cis*-hexatriene shows that the molecule is planar, despite significant H–H repulsion. The substitution method was applied to the equilibrium rotational constants to give a semiexperimental equilibrium structure for the C₆ backbone. This structure and one predicted with the B3LYP/cc-pVTZ model show structural evidence for increased π -electron delocalization in comparison with butadiene, the first member of the polyene series.

Introduction

Hydrocarbon polyenes with their conjugated double bonds play crucial roles in biological chemistry. Polyenes are important in vision, in light gathering for photosynthesis, and in pigments. Polyenes are also involved in organic electronic conductors. Chemists understand that electronic excitation energy is transmitted through the conjugated double bond system and presume that the extent of π -electron delocalization increases with chain length. Although much is known about the electronic spectroscopy of polyenes, which is consistent with increasing π -electron delocalization with chain length,¹ little is known about the bond lengths of the shorter polyenes. The object of the present investigation was to test the expectation that greater π -electron delocalization, as reflected in structural adjustments, occurs in 1,3,5-hexatriene in comparison with 1,3-butadiene.

We focus on *cis*-hexatriene (cHTE) because it has a permanent dipole moment and thus is subject to structural investigation by microwave spectroscopy. The nonpolar trans isomer, which is lower in energy by approximately 8.0 kJ/mol,^{2,3} is microwave silent.

It is now practical to obtain semiexperimental equilibrium r_e structures for medium-sized molecules. Such structures are obtained by fitting equilibrium rotational constants obtained from ground-state rotational constants derived from rotational spectroscopy and quantum chemical calculations of vibration–rotation constants (so-called spectroscopic alphas).^{4,5} Bond lengths for these structures appear to be good to ± 0.001 Å, and bond angles to $\pm 0.1^\circ$.^{4,5}

Recent work has shown that CC bond lengths in 1,3-butadiene (BDE), the first member of the polyene series, reflect adjustments in the formal C–C and C=C bond lengths in comparison with corresponding localized bond lengths.⁵ Although ethylene

is a reasonable choice for a localized C=C bond length, this molecule lacks some of the atom crowding of BDE. To date, no convincing structural data exists for a stable molecule with a naked sp²–sp² single bond.^{6,7} To obtain improved data for localized C=C and C–C(sp–sp²) bonds, the structure of 90°-twisted BDE was computed recently at a high level of theory with CCSD(T)/aug-cc-pVnZ models and a complete basis set extrapolation.⁶ In 90°-twisted BDE, the p-orbitals are essentially orthogonal. Hence, π -electron delocalization is blocked, and the species has localized C=C and sp²–sp² bonds. In 90°-twisted BDE, the length obtained for the localized C=C bond is 1.333 Å, which can be compared with 1.3305 Å for ethylene,⁵ and the length obtained for the sp²–sp² single bond is 1.482 Å, which can be compared with 1.470 Å estimated earlier from the near-equilibrium structures of ethane and propylene.⁵ In the semiexperimental equilibrium structure of BDE, the formal C=C bond lengths are 1.338 Å, and the formal sp²–sp² bond length is 1.454 Å. Thus, the increased length of the C=C bonds and the decreased length of the C–C bond reflect some π -electron delocalization.

The bond lengths and bond angles in the semiexperimental equilibrium structure of BDE and the computed equilibrium structure of cHTE are shown in Figure 1. The structure of cHTE was computed with Gaussian 03 software (G03)³ and the DFT method for the B3LYP/cc-pVTZ model with an Ultrafine grid. For comparison, predictions for butadiene with the B3LYP/cc-pVTZ model (without an Ultrafine grid) are within 0.002 Å except for the “C=C” bond, which is within 0.004 Å.⁵ The prediction for cHTE is consistent with the expectation that the central C=C bond in HTE has lengthened more than the C=C bonds in BDE in comparison with a localized C=C bond. The slightly shorter C=C length for the end C=C bonds in HTE in comparison with BDE is presumed to be a deficiency in the calculated structure. The pattern in CH bond lengths in HTE is similar to the pattern in BDE. The calculated dipole moment

[†] University of Virginia.

[‡] Universidad de Valladolid.

[§] Oberlin College.

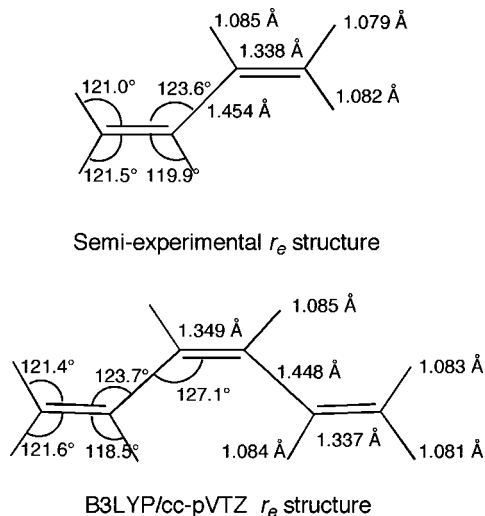


Figure 1. Semiexperimental equilibrium structure for butadiene and DFT-predicted structure for *cis*-hexatriene. Localized C=C length is 1.333 Å; localized sp²–sp² single bond length is 1.482 Å.

for cHTE is only 0.05 D. This small dipole moment presented an experimental challenge especially for observing microwave transitions for the ¹³C species in natural abundance. Observing lines for the ¹³C species was essential to obtaining structural information for the C₆ backbone.

The initial microwave survey of cHTE was done with the new technique of broad-band, chirped-pulse Fourier transform spectroscopy. The rest of the investigation was carried out with the established tuned-cavity, Fourier transform method. In both instruments, samples were introduced with the pulsed-jet method to give spectral transitions at a temperature near 1 K.

Experimental Section

Synthesis. A mixture of the two isomers of HTE was prepared at room temperature by vacuum-distilling 1,5-hexadien-3-ol

(Aldrich) through a column (2.0 cm × 30 cm) packed with phosphorus pentoxide (Aldrich) dispersed on glass wool. To obtain material free of alcohol precursor, the initial product had to be passed a second time through a freshly packed column. The yield from this method is no more than 15%, but the *cis* content is about two-thirds. Because the *trans* isomer is microwave silent, the isomer mixture can be used directly for microwave studies. The *cis* and *trans* isomers can be separated at 60 °C with two passes through a 7-m column (3/8-in) packed with 15% by weight 2-cyanoethyl ether (Aldrich) coated on Chromosorb P regular 45–60 mesh (Analabs).⁸

Two other methods were tried for preparation of cHTE. *trans,trans*-2,4-Hexadien-1-ol is also available commercially (Aldrich). However, distilling this material through a column packed with phosphorus pentoxide yields only the *trans* isomer. Mechanistic considerations show why the two alcohols give different outcomes for the isomers of HTE. For microwave spectroscopy, dehydration with phosphorus pentoxide has a distinct advantage over the method of distilling the alcohol through a column packed with aluminum oxide at temperatures near 330 °C.⁹ At these temperatures, cHTE is wasted by formation of 1,3-cyclohexadiene, and the ratio of *cis*/*trans* isomers is much less than one.

Microwave Spectroscopy. The broad-band (7.5–18.5 GHz) chirped-pulse, Fourier transform microwave (MW) spectrometer with jet-beam-cooling of the sample has been described in detail.¹⁰ For the experiments reported here, the excitation pulse was applied with a linear sweep in 1 μs, and the FID was acquired for 20 μs after a delay of 3 μs. The repetition rate was 3.5 Hz. Ten thousand scans were accumulated in 45 min.

After an initial search for a spectrum with the broad-band instrument, all further MW measurements were done on a mini Balle-Flygare-type tuned-cavity Fourier transform instrument with jet-beam-cooled sample introduction.¹¹ Separate 1 W amplifiers provided MW pulses in the 9–18 and 18–26 GHz

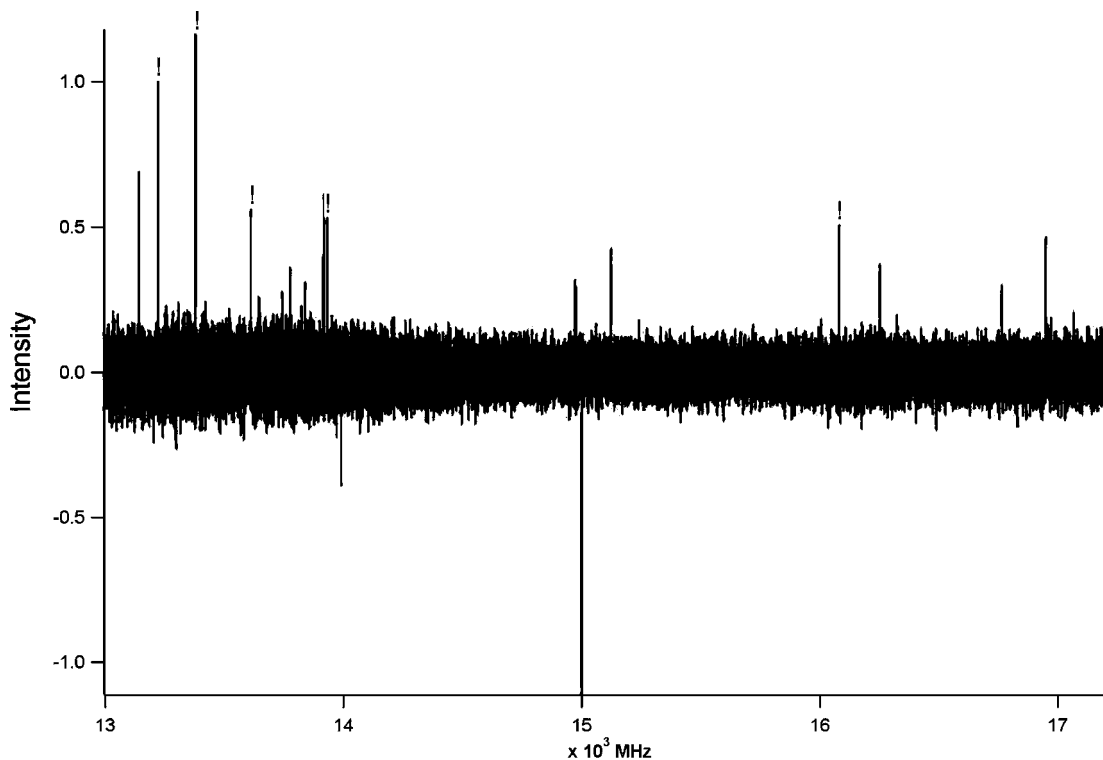


Figure 2. Broad-band microwave spectrum observed with the chirped-pulse FT instrument; 10 000 accumulations. “!” marks lines from *cis*-hexatriene.

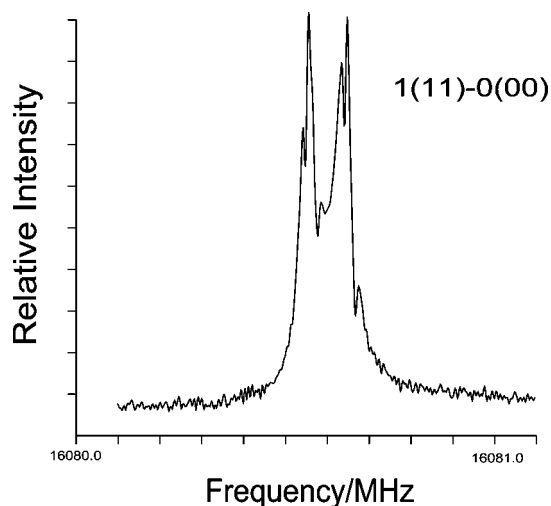


Figure 3. Microwave Doppler doublet for the $1_{11}-0_{00}$ transition of *cis*-hexatriene observed with the FT minicavity spectrometer; 1013 shots.

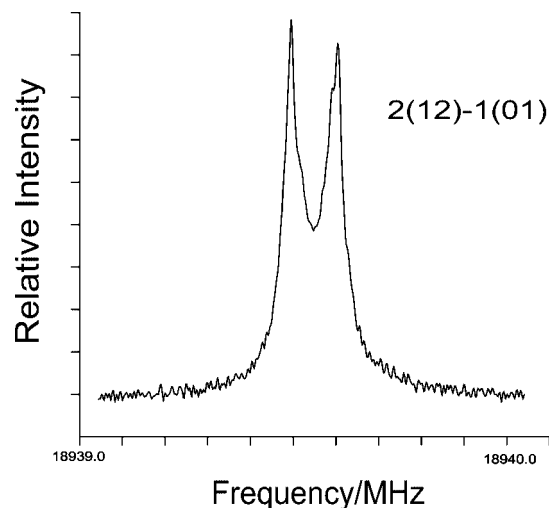


Figure 4. Microwave Doppler doublet for the $2_{12}-1_{01}$ transition of *cis*-hexatriene observed with the FT minicavity spectrometer; 100 shots.

regions. The temperature of the sample for the measurements with both instruments was estimated to be 1 K.

For the initial experiments with cHTE on the broad-band and cavity instruments, a sample of 1.9 mmol of pure cHTE mixed with 2 atm of 80% neon/20% helium driver gas in a 4-L stainless steel tank was used. For the remainder of the experiments, which included the investigation of the ^{13}C isotopomers, 13 mmol of a 2/1 mixture of *cis* and *trans* isomers was used for a gas mixture prepared in the 4-L tank with 5.4 atm of the neon–helium mixture.

Results

The dipole moment of cHTE was estimated to be only 0.05 D in the DFT calculations. The dipole moment coincides with the C_2 symmetry axis and the b principal rotation axis. Thus, all MW transitions are b -type with $\Delta J = 0, \pm 1$; $\Delta K_a = \pm 1$; $\Delta K_c = \pm 1$. The initial search for MW transitions of cHTE was made with the broad-band chirped-pulse instrument. The spectrum observed is shown in Figure 2. Part of a Q-branch series between 13 and 14 GHz was recognized from its quadratic spacing. In addition, a single R-branch transition was observed near 16 GHz. These lines are marked with “!” in Figure 2. Other impurity lines appear in this weak spectrum with its modest S/N ratio. However, the five identified lines were sufficient to get the assignment started.

Figures 3 and 4 show examples of lines observed for the normal species of cHTE with the cavity instrument. Figure 3 is the $1_{11}-0_{00}$ ($J'_{Ka'Kc'}-J''_{Ka''Kc''}$) transition observed with 1013 shots. The doubling of the lines is a consequence of the Doppler effect acting on the sample beam, which is introduced through one mirror and propagates in one direction, whereas the MW pulse is propagating in both directions as a consequence of reflection from the two mirrors. The observed frequency is the average of the Doppler doublet. Figure 4 shows the $2_{12}-1_{01}$ transition observed with 100 shots. Table 1 contains all 25 transitions observed for the normal species and the differences between the observed and calculated values. The calculated values came from the predictions of the Watson-type rotational Hamiltonian,¹² to which the data were fitted. A full set of quartic centrifugal distortion constants was used. All but δ_K were fitted to the experimental data. For δ_K the value computed with G03 and the B3LYP/cc-pVTZ model was held fixed. Table 2 gives the rotational constants fitted to the Hamiltonian with the

TABLE 1: Microwave Lines Observed for *cis*-Hexatriene

J'	K_a'	K_c'	J''	K_a''	K_c''	freq/MHz	obsd – calcd
8	0	8	7	1	7	12 863.096	−0.0001
1	1	0	1	0	1	13 221.669	−0.0042
2	1	1	2	0	2	13 376.758	0.0004
3	1	2	3	0	3	13 611.907	0.0012
4	1	3	4	0	4	13 930.130	0.0009
5	1	4	5	0	5	14 335.412	0.0001
6	1	5	6	0	6	14 832.670	−0.0027
7	1	6	7	0	7	15 427.701	0.0006
1	1	1	0	0	0	16 080.601	0.0019
8	1	7	8	0	8	16 127.057	0.0011
6	2	5	7	1	6	16 222.102	−0.0003
9	0	9	8	1	8	16 356.579	−0.0010
9	1	8	9	0	9	16 937.930	−0.0007
10	1	9	10	0	10	17 867.955	0.0005
7	2	5	8	1	8	18 311.830	−0.0004
11	1	10	11	0	11	18 924.946	−0.0002
2	1	2	1	0	1	18 939.540	−0.0021
5	2	4	6	1	5	19 760.365	−0.0009
10	0	10	9	1	9	19 879.510	−0.0010
6	2	4	7	1	7	20 618.654	−0.0005
3	1	3	2	0	2	21 722.142	0.0017
5	2	3	6	1	6	23 034.846	0.0021
4	2	3	5	1	4	23 225.938	0.0000
11	0	11	10	1	10	23 422.667	0.0011
4	1	4	3	0	3	24 430.092	0.0007

asymmetric top reduction and the F representation. The fit of the lines (Table 1) is excellent with deviations falling within 3 kHz, which is within the 4 kHz estimated experimental uncertainty in measuring lines. For structure fitting, we are particularly interested in the ground-state A , B , and C constants.

Table 3 contains the transitions observed with the cavity instrument for the three ^{13}C isotopomers in natural abundance (50 times weaker than for the normal species). Owing to the weak spectra for the ^{13}C species, the number of lines observed for each ^{13}C species was too few to fit quartic centrifugal distortion constants. For these species we used centrifugal distortion constants computed with the DFT model for each ^{13}C isotopomer and the normal species to construct factors for scaling the observed centrifugal distortion constants of the normal species. These adjusted quartic centrifugal distortion constants were held constant while fitting the microwave transitions. Table 2 contains the rotational constants for the ^{13}C isotopomers in comparison to those for the normal species.

TABLE 2: Ground-State Rotational Constants for *cis*-Hexatriene and Its ¹³C Isotopomers

	cHTE	cHTE-1- ¹³ C ₁	cHTE-2- ¹³ C ₁	cHTE-3- ¹³ C ₁
A/MHz	14 651.229 2(7)	14 606.201(1)	14 581.503(1)	14 411.130(3)
B/MHz	1 583.181 4(1)	1543.538(1)	1571.686(1)	1580.989(1)
C/MHz	1 429.461 9(1)	1396.653 9(4)	1419.433 1(4)	1425.350 4(7)
δ _J /kHz	0.028 6(2)	0.026 8 ^a	0.028 3 ^a	0.028 8 ^a
δ _K /kHz	0.643 ^b	0.618 ^a	0.638 ^a	0.637 ^a
Δ _K /kHz	102.9(2)	104.1 ^a	100.1 ^a	101.6 ^a
Δ _{JK} /kHz	-5.06(3)	-4.96 ^a	-5.01 ^a	-4.98 ^a
Δ _J /kHz	0.162(1)	0.154 ^a	0.162 ^a	0.161 ^a
κ	-0.976 75	-0.977 76	-0.976 86	-0.976 03
s. d./kHz	1.67	2.28	2.66	3.78
no. lines	25	8	8	7
Δ/u Å ²	-0.166 4	-0.166 5	-0.168 2	-0.163 9

^a Gaussian 03 with B3LYP/cc-pVTZ(Ultrafine grid) predictions scaled to normal. ^b Gaussian 03 with B3LYP/cc-pVTZ(Ultrafine grid) prediction.

TABLE 3: Microwave Lines Observed for the ¹³C Isotopomers of *cis*-Hexatriene

J'	K _a '	K _c '	J''	K _a ''	K _c ''	freq/MHz	obsd - calcd
1- ¹³ C ₁							
1	1	0	1	0	1	13 209.449	-0.0025
2	1	1	2	0	2	13 357.583	-0.0006
3	1	2	3	0	3	13 582.087	0.0013
4	1	3	4	0	4	13 885.709	-0.0011
1	1	1	0	0	0	16 002.764	0.0027
2	1	2	1	0	1	18 796.089	0.0011
3	1	3	2	0	2	21 516.445	0.0015
4	1	4	3	0	3	24 165.376	-0.0024
2- ¹³ C ₁							
1	1	0	1	0	1	13 161.978	-0.0001
2	1	1	2	0	2	13 315.579	0.0028
3	1	2	3	0	3	13 548.460	0.0020
4	1	3	4	0	4	13 863.590	-0.0014
1	1	0	0	0	0	16 000.842	-0.0045
2	1	2	1	0	1	18 839.732	0.0002
3	1	3	2	0	2	21 602.998	-0.0001
4	1	4	3	0	3	24 292.319	0.0011
3- ¹³ C ₁							
2	1	1	2	0	2	13 142.750	0.0007
3	1	2	3	0	3	13 380.976	0.0006
4	1	3	4	0	4	13 703.502	-0.0059
5	1	4	5	0	5	14 114.507	0.0031
2	1	2	1	0	1	18 687.112	0.0023
3	1	3	2	0	2	21 460.549	0.0014
4	1	4	3	0	3	24 158.474	-0.0022

Though a bit larger than for the normal species, the obsd - calcd differences for the ¹³C species in Table 3 are quite good.

Included in Table 2 are the inertial defects for the four species. The inertial defect is defined as $\Delta = I_c - I_a - I_b$, where I_c is the moment of inertia around the *c* principal rotation axis and the other two are for the *a* and *b* axes. The small values for Δ for each species confirm that cHTE is a planar molecule despite the repulsion of the H2 and H5 hydrogen atoms.

The possibility of observing MW lines for two other planar rotamers of c-HTE was considered. One rotamer with C_s symmetry has the C1C2 double bond rotated 180°. The other with C_{2v} symmetry has both the C1C2 and C5C6 double bonds rotated 180°. Predictions with the B3LYP/cc-pVTZ model gave energies of 23 kJ/mol for the C_s rotamer and 53 kJ/mol for the C_{2v} rotamer relative to the structure shown in Figure 1. Both of these rotamers had imaginary frequencies and thus were transition states. Nonplanar rotamers were not explored.

Discussion

Having only ground-state rotational constants for the normal species and the ¹³C species, a full structural analysis for cHTE

TABLE 4: Equilibrium Rotational Constants for *cis*-Hexatriene and Its Three ¹³C Isotopomers

	normal	1- ¹³ C ₁	2- ¹³ C ₁	3- ¹³ C ₁
A/MHz	14 820.964	14 775.689	14 750.094	14 576.415
B/MHz	1 591.007	1 551.112	1 579.411	1 588.763
C/MHz	1 436.920	1 403.891	1 426.796	1 432.761
Δ ^a /u Å ²	-0.036 3	-0.036 1	-0.036 8	-0.036 2

^a Inertial defect, $\Delta = I_c - I_a - I_b$.

cannot be done at present. However, the ground-state rotational constants for the normal species and the ¹³C isotopomers enable structure fitting for the C₆ backbone, which is of particular interest. Standard practice in MW spectroscopy is to use ground-state rotational constants in the Kraitchman substitution method to find the Cartesian coordinates of the substituted atoms in the principal axis system of the normal species.¹³ This strategy gives structural parameters intermediate between a strictly ground-state structure and the equilibrium structure, in which all of the atoms are at rest. The equilibrium structure is the one computed by ab initio methods. We applied the substitution method to the ground-state rotational constants and obtained the following bond parameters: C1C2, 1.343 Å; C2C3, 1.457 Å; C3C4, 1.335 Å; C1C2C3, 123.2°; C2C3C4, 126.5°. The bond lengths were disappointing in comparison with qualitative expectations and the results of the DFT calculations shown in Figure 1. The C1C2 “double” bond length is longer than the C3C4 “double” bond length. The C2C3 “single” bond was longer than in BDE. Of course, the fuzziness of atom positions caused by zero point vibrations in the ground-state contributes to an r_s structure of this type.

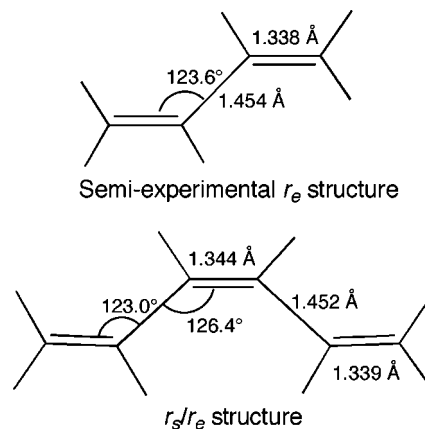


Figure 5. r_s/r_e structure for the C₆ backbone of *cis*-hexatriene compared with the semiexperimental structure for the C₄ backbone of butadiene.

A new strategy was applied to finding coordinates of the carbon atoms, which we call an r_s/r_e structure. In this strategy, equilibrium rotational constants were found for the normal species and the three ^{13}C species from the ground-state rotational constants and vibration-rotation constants (alphas). Then, an r_s analysis¹³ was applied to the equilibrium rotational constants to obtain Cartesian coordinates for the carbon atoms in the principal axis system of the parent. This method was tested with butadiene. Equilibrium rotational constants from Table 6 (for the B3LYP/cc-pVTZ model) in ref 5 were used in an r_s/r_e analysis for the C_4 backbone of butadiene. The results gave a “C=C” bond length of 1.338 Å, a “C-C” bond length of 1.454 Å, and a C=C-C bond angle of 123.5°. These values agree closely with the accepted semiexperimental values of 1.338 Å, 1.454 Å, and 123.6°.⁵ As part of the semiexperimental structural study of butadiene, different models for computing the alphas were explored. The semiexperimental structure was largely insensitive to differences in alphas from the various models.

For cHTE the alphas were computed by G03 with the B3LYP/cc-pVTZ model. For the three ^{13}C species, which lack full C_{2v} symmetry, care was taken to have G03 do this calculation in the principal axis system of each ^{13}C species.¹⁴ We also computed the alphas for the normal species with the higher level B3LYP/aug-cc-pVTZ model. The small differences from the results with the simpler cc-pVTZ basis set did not justify recomputing alphas with the “aug” enhancement for the ^{13}C species. Table 4 gives the equilibrium rotational constants for cHTE computed in this way. The inertial defect Δ 's, which in a true equilibrium structure would be zero, are about five times smaller than those for the ground state (Table 2). Figure 5 shows the results for the C_6 backbone with the r_s/r_e structure. While not the last word for a semiexperimental structure for cHTE, these results are qualitatively reasonable and compare favorably with the DFT predictions in Figure 1. We see that the central C=C bond has lengthened appreciably with respect to a localized C=C bond and the C=C bond in BDE. The end C=C bonds are slightly longer than the C=C bonds in BDE in contrast to the DFT prediction. The C2C3C4 bond angle is appreciably larger than the C1C2C3 bond angle, which is close to the angle in BDE. The increase in the C2C3C4 angle is an accommodation to the repulsion of the H2 and H5 hydrogen atoms.

Until rotational constants are obtained for a full set of deuterium isotopomers, the semiexperimental structure for cHTE remains provisional. An improved fitting strategy consists of a simultaneous global fit to equilibrium rotational constants for a full set of isotopomers, which provides a greater constraint on the resulting Cartesian coordinates. The substitution strategy depends on relatively small differences between moments of inertia for the normal species and each isotopomer. These differences can become quite small and introduce large uncertainties for atoms close to the principal rotation axis. Fortunately, none of the carbon atoms in cHTE is close to a rotation axis.

We are currently working on syntheses of deuterium-substituted isotopomers of HTE. A parallel investigation of the

structure of tHTE is proceeding with ground-state rotational constants being derived from the analysis of rotational structure in the high-resolution infrared spectra of this nonpolar substance.

Acknowledgment. We are grateful to a reviewer for suggesting the test of the r_s/r_e method on butadiene. A.L. received support from the Programa Nacional de Ayudas para la Movilidad in Spain. NSF grant CRIF: ID CHE-0618755 supported the work at Virginia. Amie K. Patchen prepared some of the pure *cis*-hexatriene. DFT calculations were done on the Beowulf cluster at Oberlin College, which was provided by NSF grant 0420717. N.C.C. and the Oberlin students were supported by a Dreyfus Senior Scholar Mentor grant.

References and Notes

- (1) Christensen, R. L.; Faksh, A.; Meyers, J. A.; Samuel, I. D. W.; Wood, P.; Schrock, R. R.; Hultsch, K. C. *J. Phys. Chem. A* **2004**, *108*, 83339–8236.
- (2) The energy difference comes from B3LYP/cc-pVTZ (Ultrafine grid) calculations.
- (3) Frisch, M. J.; Trucks, G. W.; Schlegel, H. B.; Scuseria, G. E.; Robb, M. A.; Cheeseman, J. R.; Montgomery, J. A., Jr.; Vreven, T.; Kudin, K. N.; Burant, J. C.; Millam, J. M.; Iyengar, S. S.; Tomasi, J.; Barone, V.; Mennucci, B.; Cossi, M.; Scalmani, G.; Rega, N.; Petersson, G. A.; Nakatsuji, H.; Hada, M.; Ehara, M.; Toyota, K.; Fukuda, R.; Hasegawa, J.; Ishida, M.; Nakajima, T.; Honda, Y.; Kitao, O.; Nakai, H.; Klene, M.; Li, X.; Knox, J. E.; Hratchian, H. P.; Cross, J. B.; Adamo, C.; Jaramillo, J.; Gomperts, R.; Stratmann, R. E.; Yazyev, O.; Austin, A. J.; Cammi, R.; Pomelli, C.; Ochterski, J. W.; Ayala, P. Y.; Morokuma, K.; Voth, G. A.; Salvador, P.; Dannenberg, J. J.; Zakrzewski, V. G.; Dapprich, S.; Daniels, A. D.; Strain, M. C.; Farkas, O.; Malick, D. K.; Rabuck, A. D.; Raghavachari, K.; Foresman, J. B.; Ortiz, J. V.; Cui, Q.; Baboul, A. G.; Clifford, S.; Cioslowski, J.; Stefanov, B. B.; Liu, G.; Liashenko, A.; Piskorz, P.; Komaromi, I.; Martin, R. L.; Fox, D. J.; Keith, T.; Al-Laham, M. A.; Peng, C. Y.; Nanayakkara, A.; Challacombe, M.; Gill, P. M. W.; Johnson, B.; Chen, W.; Wong, M. W.; Gonzalez, C.; Pople, J. A. *Gaussian 03*, revision C.02; Gaussian, Inc.: Wallingford, CT, 2004.
- (4) Demaison, J.; Rudolph, H. D. *J. Mol. Spectrosc.* **2008**, *248*, 66–76.
- (5) Craig, N. C.; Groner, P.; McKean, D. C. *J. Phys. Chem. A* **2006**, *110*, 7461–7469.
- (6) Feller, D.; Craig, N. C.; Matlin, A. R. *J. Phys. Chem. A* **2008**, *112*, 2131–2133.
- (7) Brain, P. T.; Smart, B. A.; Robertson, H. E.; Rankin, D. W. H.; Henry, W. J.; Gosney, I. *J. Org. Chem.* **1997**, *62*, 27672773. Although [4]-dendralene, a dimer of butadiene, is a real molecule that presumably has a naked $\text{sp}^2\text{-sp}^2$ bond between the two butadiene moieties, the bond length of 1.497 Å found for the $\text{sp}^2\text{-sp}^2$ bond in an electron diffraction study is close to the $\text{sp}^2\text{-sp}^3$ bond in propylene, which is 1.496 Å (ref 4).
- (8) Hwa, J. C. H.; de Bennerville, P. L.; Sims, H. J. *J. Am. Chem. Soc.* **1960**, *82*, 2537–2540.
- (9) Woods, G. F.; Schwartzman, L. H. *J. Am. Chem. Soc.* **1948**, *70*, 3394–3396.
- (10) Brown, G. G.; Dian, B. C.; Douglass, K. O.; Gener, S. M.; Shipman, S. T.; Pate, B. H. *Rev. Sci. Instrum.* **2008**, *79*, 053103.
- (11) Suenram, R. D.; Grabow, J. U.; Zuban, A.; Leonov, I. *Rev. Sci. Instrum.* **1999**, *70*, 2127–2135.
- (12) Gordy, W.; Cook, R. L. *Microwave Molecular Spectra, Techniques of Organic Chemistry*, 3rd ed.; Weissberger, A., Ed.; John Wiley & Sons: New York, 1984; Vol. XVIII, p 331.
- (13) Ref 12, p 661.
- (14) McKean, D. C.; Craig, N. C.; Law, M. M. *J. Phys. Chem. A* **2008**, *112*, 6760–6771.

JP8106777